JACS
JOURNAL OF THE AMERICAN CHEMICAL SOCIETY

Article

pubs.acs.org/JACS

A pH-Induced Switch in Human Glucagon-like Peptide-1 Aggregation Kinetics

Karolina L. Zapadka,[†] Frederik J. Becher,[†] Shahid Uddin,[‡] Paul G. Varley,[‡] Steve Bishop,[∥] A. L. Gomes dos Santos,[‡] and Sophie E. Jackson*[,†]

[†]Department of Chemistry, University of Cambridge, Cambridge CB2 1EW, U.K.

[‡]Formulation Sciences, MedImmune Ltd., Granta Park, Cambridge CB21 6GH, U.K.

[∥]Formulation Sciences, MedImmune, One MedImmune Way, Gaithersburg, Maryland 20878, United States

Supporting Information

ABSTRACT: Aggregation and amyloid fibril formation of peptides and proteins is a widespread phenomenon. It has serious implications in a range of areas from biotechnological and pharmaceutical applications to medical disorders. The aim of this study was to develop a better understanding of the mechanism of aggregation and amyloid fibrillation of an important pharmaceutical, human glucagon-like peptide-1 (GLP-1). GLP-1 is a 31-residue hormone peptide that plays an important role regulating blood glucose levels, analogues of which are used for treatment of type 2 diabetes. Amyloid fibril formation of GLP-1 was monitored using thioflavin T fluorescence as a function of peptide concentration between pH 7.5 and 8.2. Results from these studies establish that there is a highly unusual pH-induced switch in GLP-1 aggregation kinetics. At pH 8.2, the kinetics are consistent with a nucleation−polymerization mechanism for fibril formation. However, at pH 7.5, highly unusual kinetics are observed, where the lag time increases with increasing peptide concentration. We attribute this result to the formation of off-pathway species together with an initial slow, unimolecular step where monomer converts to a different monomeric form that forms on-pathway oligomers and ultimately fibrils. Estimation of the pK_a values of all the ionizable groups in GLP-1 suggest it is the protonation/deprotonation of the N-terminus that is responsible for the switch with pH. In addition, a range of biophysical techniques were used to characterize (1) the start point of the aggregation reaction and (2) the structure and stability of the fibrils formed. These results show that the off-pathway species form under conditions where GLP-1 is most prone to form oligomers.

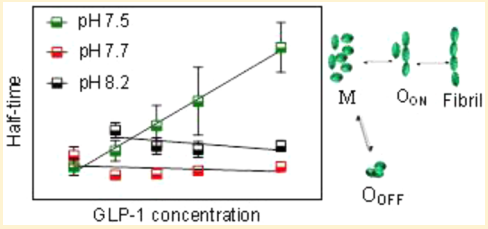

INTRODUCTION

The aggregation of peptides and proteins into β-sheet rich amyloid fibrils is a common process increasingly associated with problems in drug development and pharmaceutical applications, as well as many disease states.[1] Although significant progress has been made over the past 15 years in elucidating the structure[2] and morphology[3] of amyloid fibrils and their mechanism of formation,[4,5] our current understanding of how peptides and proteins aggregate into fibrils remains incomplete. It has been shown that amyloid fibrils are commonly formed through a nucleation−polymerization (N−P) mechanism with characteristic sigmoidal-like kinetics. There is an initial lag phase, during which critical nucleating species are formed, which is followed by a rapid growth phase, and then a plateau as either the system reaches equilibrium or the monomer levels are completely depleted.[6,5]

Oligomers have often been observed to form during fibril formation, albeit at sometimes very low concentrations.[7,8] However, many aspects of the relationship between oligomers and the mechanism of fibril formation are not yet fully understood.[8] Considerable progress has been made in understanding some of the factors affecting the aggregation propensity of a system, which has been shown to depend upon sequence, monomer conformation, nucleation rate, effective monomer concentration, pH, ionic strength, small molecules, and external factors such as temperature or agitation.[5,9,10]

In this work, we focus on the human glucagon-like peptide-1, GLP-1(7−37), which is a 31-residue hormone peptide.[11] GLP-1 plays an important role in our body regulating blood glucose levels through regulation of glucose-dependent insulin secretion, inhibition of glucagon secretion, and gastric emptying together with reduction of food intake.[11] It is an important pharmaceutical molecule, analogues of which are used for the treatment of type 2 diabetes.[11,12] It has previously been reported that GLP-1 aggregates into amyloid fibrils under physiological conditions[13] and at pH 5.8.[14]

Here, we present the results of a detailed study of the pH dependence of the aggregation kinetics of GLP-1. Aggregation kinetics were monitored by thioflavin T (ThT), which increases its fluorescence upon binding to β-sheet rich amyloid fibrils.[5] Kinetic data from these experiments were analyzed to obtain the apparent growth rate, $t_{1/2}$, and lag time at different peptide concentrations and pH values.

Received: June 1, 2016
Published: November 10, 2016

DOI: 10.1021/jacs.6b05025
J. Am. Chem. Soc. 2016, 138, 16259−16265

We report an unusual pH-induced switch in GLP-1 aggregation kinetics.

In order to understand the complex, pH-dependent aggregation kinetics obtained, a detailed characterization of freshly prepared samples of GLP-1 was undertaken using a range of biophysical techniques to obtain information on the size, structure, and oligomeric state of species present. This included analytical ultracentrifugation (AUC), asymmetric flow field-flow fractionation (AF4) with multiangle light scattering detector (MALS), dynamic light scattering (DLS), size-exclusion chromatography (SEC), far-UV circular dichroism (far-UV CD), and ANS-binding assays. In all cases, fibrils formed were confirmed using atomic force microscopy (AFM) and transmission electron microscopy (TEM) providing information on the structure, stability, and morphology of the fibrils and how this depends upon pH.

EXPERIMENTAL SECTION

Materials. The 31-residue GLP-1(7−37) (HAEGTFTSDVSSYLEGQAAKEFIAWLVKGRG) was purchased from Bachem (98.5% pure), with a molecular weight of 3.36 kDa and used without further purification. GLP-1 powder was dissolved in buffer (25 mM sodium phosphate at pH 7.5 or 25 mM Tris-HCl at pH 8.0 or 8.5) to a final concentration of 298 μM. The solution was filtered (0.22 μm filter) prior to use, and the concentration was determined spectrophotometrically using a NanoDrop spectrophotometer (ND 2000, Thermo Scientific) and a theoretical extinction coefficient of 6990 M^{-1} cm^{-1} at 280 nm. All other chemicals were of analytical grade.

Kinetics of Aggregation: Thioflavin T Binding Assays. For kinetic experiments, a stock solution of 298 μM GLP-1 in buffer was prepared, as described above. Final concentrations of GLP-1 were 25, 50, 75, 100, and 150 μM, and the samples were incubated with 50 μM ThT and 0.01% NaN_3 (added to prevent bacterial growth). The 50 μM concentration for ThT was chosen as the aggregation kinetics were shown to be independent of ThT concentration between 10 and 80 μM ThT, Figure S1. The peptide/ThT samples (120 μL) were pipetted into a 96-well half-area plate made of black polystyrene with a clear bottom and a nonbinding surface (Corning 3881, USA). A sealing tape (Costar Thermowell) was used to protect samples from evaporation. Fluorescence measurements were carried out on a Fluorostar Optima Microplate Reader (BMG Labtech, Offenburg, Germany), which was thermostated at 37 °C. ThT binding to fibrils was monitored by using an excitation filter at 440 nm and recording the fluorescence emission at 480 nm. Bottom reading of the plate every 30 min with 5 min of shaking prior to each measurement was performed. Each cycle was executed with the orbital shaker at 350 rpm, 5 flashes per well, and fluorescence measurements were made at a gain of 1000.

Each individual ThT data set was fit to eq 1,

$$y = y_0 + A/(1 + \exp(-k(t - t_{1/2}))) + bt \quad (1)$$

where y_0 is the starting fluorescence, A is the amplitude of the transition, $t_{1/2}$ is the half-time, which is defined as the time at which the ThT fluorescence has reached 50% of its final baseline value, k is the apparent growth rate, and b is the slope of the final baseline. Note in many other studies, data are normalized prior to fitting such that the inclusion of this additional term is not needed. The lag time was calculated from the kinetic parameters obtained using eq 2:[15,20]

$$t_{lag} = t_{1/2} - 2/k \quad (2)$$

All measurements were made in triplicate for each peptide concentration in a single 96-well plate, and each experiment was repeated at least three times on different days with freshly prepared samples.

Analytical Ultracentrifugation (AUC) Sedimentation Velocity Experiment. Sedimentation velocity measurements were performed at 20 °C, 60 000 rpm using a Beckman Optima XL-I analysis ultracentrifuge equipped with an An-60Ti rotor. The instrument was equipped with a UV−visible absorbance detector. GLP-1 (150 μM) was prepared in buffer and incubated at room temperature for 2 h before the start of the experiment. The sample (400 μL) was loaded into the AUC cell. The SEDFIT program was used to correct the sedimentation coefficient distributions to standard conditions, and the c(s) method was implemented (www.analyticalultracentrifugation.com/default.htm).

Asymmetric Flow Field-Flow Fractionation with Multiangle Light Scattering (AF4-MALS). AF4-MALS was used to separate and estimate the size of species in a 1500 μM solution of freshly prepared GLP-1 sample in buffer using an Eclipse (Wyatt Technology Europe GmbH, Dernbach, Germany). The AF4 was controlled by a high-performance liquid chromatography system (HPLC, Agilent) equipped with UV/vis and MALS detectors (Wyatt Technology Europe GmbH, Dernbach, Germany). A 1 kDa cutoff poly(ether sulfone) (PES) membrane was used in the Eclipse SC channel for optimal separation of species (Pall, New York, USA). Buffer was used as the mobile phase, and the system was equilibrated overnight prior to the experiment. The channel flow was maintained at 1 mL min^{-1}, and the cross-flow was varied: 4.5 mL min^{-1} from 0 to 2 min, 2.5 mL min^{-1} from 2 to 5 min, 4.5 mL min^{-1} from 5 to 15 min, 4 mL min^{-1} from 15 to 20 min then 1 mL min^{-1} from 20 to 30 min. Detection was accomplished using UV absorbance at 280 nm and multiangle light scattering. Data from MALS were analyzed by ASTRA (Wyatt Technology Europe GmbH, Dernbach, Germany). The detectors were calibrated using BSA standards (Thermo Scientific). The calibration was validated by separation of 25 μL of 2 mg mL^{-1} BSA in an appropriate mobile phase.

Dynamic Light Scattering (DLS). The intensity-weighted mean hydrodynamic diameter distribution and the number size distribution of freshly prepared GLP-1 (1500 μM) and fibrillar GLP-1 (1500 μM) in buffer at room temperature (20−25 °C) were determined by DLS using a Zetasizer Nano ZS (Malvern Instruments, Malvern, U.K.). A Zen 2112 cuvette and a scattering angle of 173° were used. The average values of the polydispersity index (PdI) were obtained from the cumulants analysis of the intensity autocorrelation function that was performed by the Zetasizer Software provided by the manufacturer. Reported parameters were determined from an average of at least three measurements.

Atomic Force Microscopy (AFM). GLP-1, from either (i) a freshly prepared solution or (ii) mature fibrils, was spread onto freshly cleaved mica (SPI supplies, West Chester, PA). The samples were then incubated for 20 min, followed by washing with 200 μL of deionized water, and dried under a stream of nitrogen. Images were acquired in air at room temperature (20−25 °C) with a PicoPlus AFM instrument with a PicoSPM II controller from Molecular Imaging (Agilent Technologies, USA) in AC mode, equipped with a MikoMasch NSC26/No Al cantilever, between 65 and 130 Hz frequency, force constant varying from 0.6 to 2.0 N m^{-1} (Innovative Solutions Bulgaria Ltd., Sofia, Bulgaria). The images were analyzed with the open source software Gwyddin (http://gwyddion.net/).[16]

RESULTS AND DISCUSSION

Aggregation Kinetics. The aggregation kinetics of amyloid fibril formation were measured starting from freshly prepared samples of GLP-1 at three different pH values using ThT fluorescence. The aggregation was monitored over a range of peptide concentrations from 25 to 150 μM. Typical results are shown in Figure 1. Kinetic parameters were determined by fitting the data to eq 1, and a lag time was then calculated for each data set using eq 2. Standard sigmoidal curves were obtained for GLP-1 aggregation under all the conditions used; however, the kinetic parameters obtained from the fitting varied with pH and peptide concentration, Figure 1. See SI2, Table S1, for further details.

At higher pH (≥8.2), the $t_{1/2}$ is found to decrease with increasing peptide concentration characteristic of a process

DOI: 10.1021/jacs.6b05025
J. Am. Chem. Soc. 2016, 138, 16259−16265

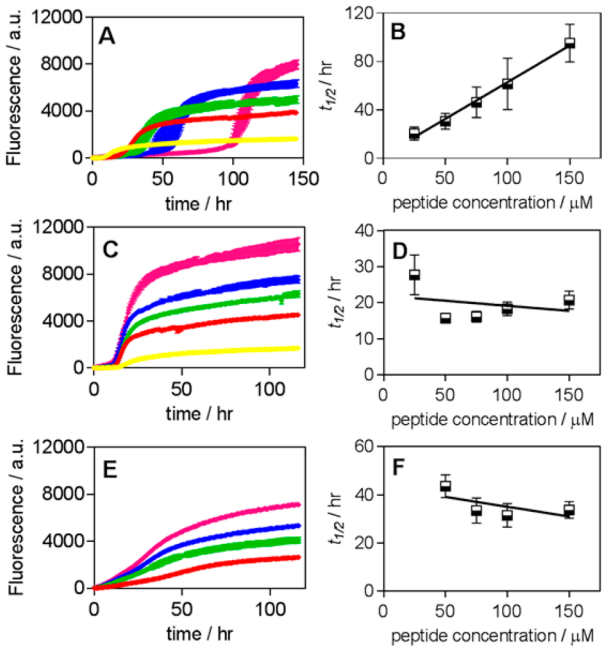

Figure 1. Aggregation kinetics of GLP-1 as a function of peptide concentration at different pHs. GLP-1 aggregation kinetics at pH 7.5 (A,B), pH 7.7 (C,D), and pH 8.2 (E,F). Panels A, C, and E show typical traces for the fibrillation of GLP-1 followed by ThT fluorescence at different GLP-1 concentrations. Each peptide concentration was run in triplicate. Panels D, E, and F show the dependence of the $t_{1/2}$ on the concentration of GLP-1. The error bars shown in panels A, C, and E are the standard deviation from the mean for a single experiment in which each peptide concentration was run in triplicate. In panels B, D and F, the error bars correspond to the standard deviations of the kinetic parameters determined from three independent experiments each of which was run in triplicate.

following a nucleation−polymerization mechanism for fibril formation, Figure 1F. Surprisingly at lower pH values there is either very little dependence on peptide concentration or the $t_{1/2}$ increases with increasing peptide concentration, Figure 1D,B. These results were very reproducible. The highly unusual kinetics were observed for GLP-1 aggregation at pH 7.5 where the $t_{1/2}$ increases with increasing peptide concentration (the opposite of what is expected for a N−P model) suggesting that other processes come into play, Figure 1B. These unusual results have, to the best of our knowledge, been observed for just two other systems: ribosomal protein S6 (where a model involving an off-pathway oligomerization process was proposed)[17] and immunoglobulin light chain (where an increase in concentration leads to a monotonic decrease in fibrillation propensity, which has been related to dimer formation in the native state).[18]

In order to assess the degree to which GLP-1 monomer is converted into amyloid fibrils in the ThT assays, monomer depletion experiments were also undertaken, SI3. Using UPLC methods (ultrapressure liquid chromatography), the loss in signal corresponding to monomeric or small soluble oligomers of GLP-1 was monitored with time, Figure S2. After 120 h at pH 7.7 at 37 °C, a solution of 75 μM GLP-1 was almost completely converted into high molecular weight species, Figure S3.

Characterization of Freshly Prepared Samples of GLP-1 in Buffer, at the Starting Point of the Kinetic Assays, at Different pH Values. A wide range of biophysical techniques were used to fully characterize the structure and properties of freshly prepared samples of GLP-1 at pH 7.5, 8.0, and 8.5. The structure of species in solution was probed using far-UV CD, and the hydrophobic surface area was probed using ANS-binding assays, while the size of species in solution was investigated using SEC, AF4, AUC, DLS, AFM, and TEM; see the following sections.

Characterization of the Structure and Hydrophobicity of Freshly Prepared GLP-1 Samples. The far-UV CD spectra of freshly prepared samples of GLP-1 show that there is no change in the secondary structure with pH, Figure S4. The average secondary structure is predicted to be approximately 30% α-helix, 20% β-strand, 20% turns, and 30% disordered between pH 7.5 and 8.5. ANS binding was also used to probe the exposed hydrophobic surface area.[19] ANS binding to freshly prepared samples of GLP-1 at different pH values was assessed using fluorescence measurements over a range of peptide concentrations, see SI5 Figure S5. The data clearly indicate that GLP-1 is more highly prone to form oligomers with exposed hydrophobic surface area at pH 7.5 relative to pH 8.0 or 8.5.

Characterization of the Size Distribution of Species in Freshly Prepared GLP-1 Samples. The size distribution of species in freshly prepared samples of GLP-1 was performed using a range of biophysical techniques from pH 7.5 to 8.5. Although standard size-exclusion chromatography was useful to give an initial assessment of the size of the major species in solution for GLP-1 at different pH values (see SI6, Figure S6), this method was unable to detect small populations of larger species. To do this, more sophisticated methods of analysis were required. Using AF4, we were successfully able to detect and separate monomeric GLP-1 from small oligomers present in the samples at both pH 8.0 and 8.5 (Figure 2C and E).

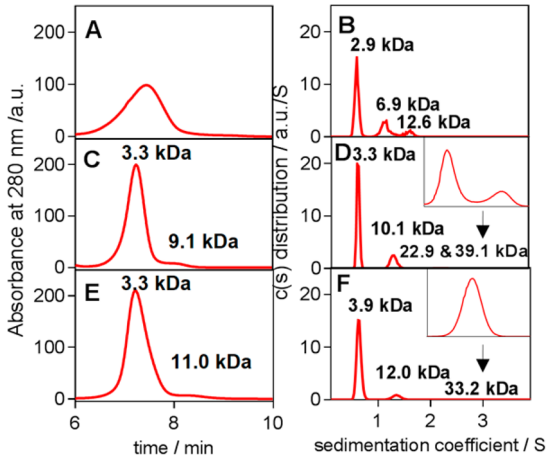

Figure 2. Size distribution of species in freshly prepared GLP-1 samples at different pHs determined using AF4 and AUC: (A,B) pH 7.5, (C,D) pH 8.0, and (E,F) pH 8.5. The left-hand column shows the AF4 results (A, C, and E) along with the M_w of monomers and small oligomers estimated using MALS (see section SI7, Figure S7, for more detail). The right-hand column shows the results of the AUC sedimentation velocity analysis of the GLP-1 samples illustrating the size distribution of sedimenting species obtained by c(s) analysis.

At pH 8.0 and 8.5, the distinct peaks observed likely correspond to a monomer and trimer with molecular weights of, 3.3 and 9.1 kDa at pH 8.0 and 3.3 and 11 kDa at pH 8.5. However, at pH 7.5, a single broad peak was observed suggesting a high level of heterogeneity of species in solution at this pH compared with the higher pHs, Figure 2A. See SI7, Figure S7, for further detail.

DOI: 10.1021/jacs.6b05025
J. Am. Chem. Soc. 2016, 138, 16259−16265

Analytical centrifugation measurements of sedimentation velocities were also performed, and as with the AF4 data, similar velocity profiles were obtained at pH 8.0 and 8.5, (Figure 2D,F). In these cases, the samples are mainly monomeric; however, small populations of both small and larger oligomers are present, Figure 2D,F, inset figures, and Table 1. Interestingly, the sedimentation velocity profile at pH 7.5 shows mainly monomer, Figure 2B; however, the sample is much more polydisperse in comparison to the results at higher pH values. At pH 7.5, larger oligomers are not present, Table 1 and Figure 2B. Molecular masses corresponding to a trimer determined using AUC were 12 kDa at pH 8.5 and 10 kDa at pH 8.0. At 7.5, oligomeric species ranged from 6.9 to 12.6 kDa corresponding to a mix of dimer, trimer, and tetramer, Figure 2. See SI7, Figure S7, for further detail.

Table 1. Percentage of Oligomeric Species Present in Freshly Prepared GLP-1 Samples[a]

	percentage of the species present (%)		
pH	monomer	small oligomers	larger oligomers
7.5	64	36	[b]
8.0	77	21.5	1.5
8.5	90	9.7	0.3

[a]For more information, see section SI10, Table S4. [b]Not observed.

Dynamic light scattering (DLS), a technique that is sensitive to large particles in solution, was also used to probe whether larger oligomeric species not detectable by AF4 or AUC are present in solution. The DLS results (Figure 3) confirmed that the main population has a small hydrodynamic radius that likely corresponds to GLP-1 monomer and the small oligomers detected by AF4 and AUC, Figure 2. However, larger particles were also found to be present under all conditions, Figure 3. These were also observed in both AFM and TEM images (see SI9, Figure S9).

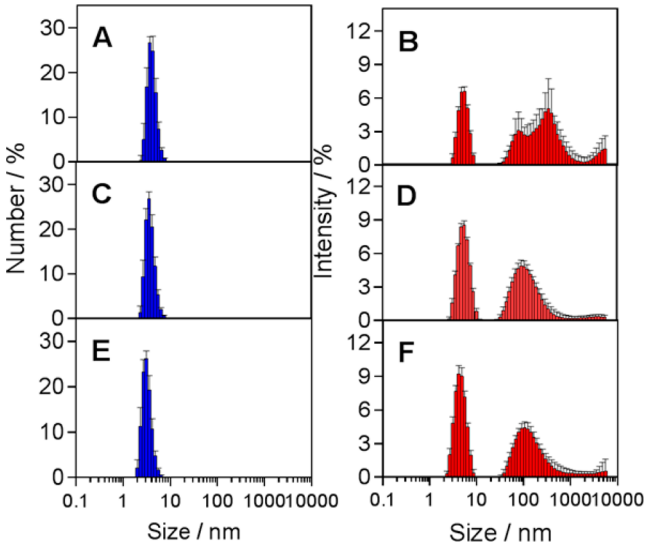

Figure 3. Dynamic light scattering results of freshly prepared GLP-1 at three different pHs: (A,B) pH 7.5, (C,D) pH 8.0, and (E,F) pH 8.5. The left-hand column shows the size distribution by number (A, C, and E), and the right-hand column shows the size distribution by intensity (B, D, and F). See section SI8, Figure S8, for more detail.

Fibril Structure and Morphology. The structure of the fibrils formed at the end of the ThT assays was investigated by far-UV CD, Figure S4C. Although the spectra recorded at the three pH values are slightly different, they all show a broad minima around 218 nm characteristic of amyloid fibrils, Figure S4C. AFM was also used to verify and characterize the fibrils formed under different conditions, Figure 4. In these cases, 150 μM GLP-1 samples at pH 7.5, 7.7, and 8.2 were allowed to aggregate at 37 °C for 200 h in the presence of 50 μM ThT and 0.01% NaN_3. Fibrils were then retrieved and imaged using AFM, Figure 4.

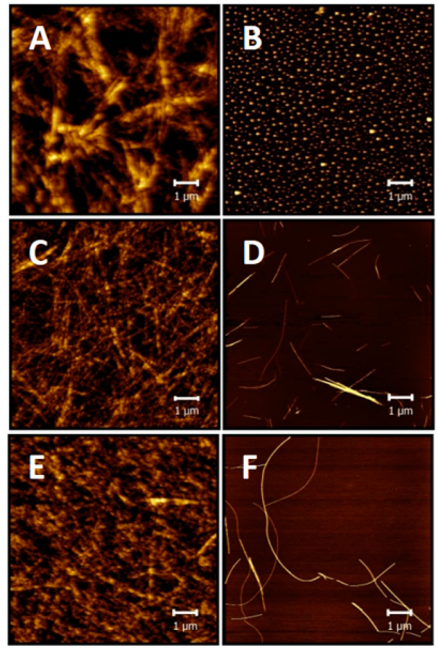

Figure 4. Atomic force microscopy images of typical GLP-1 fibrils formed under different conditions: (A,B) pH 7.5, (C,D) pH 8.0, and (E,F) pH 8.5. The left-hand column shows AFM images of samples of 150 μM GLP-1 aggregated for 200 h at 37 °C. The right-hand column shows AFM images of the fibrils diluted 100 times into deionized water prior to imaging (see section SI11, Figure S10, for more details).

Fibrils formed at 37 °C, pH 7.7 and 8.2, are stable and typically 1−3 μm in length and 10−15 nm in height, and have a twist (Figure 4 and SI11, Figure S10). In contrast, the fibrils formed at pH 7.5 are short, thin, sticky, and considerably more heterogeneous, Figure 4. In addition, at pH 7.5, fibrils are unstable and dissociate after dilution (100-fold) either in water or buffer, Figure 4B (see SI11, Figure S10, for more detail). After dilution spherical-like morphologies are observed with diameters ranging from 0.1 to 0.4 μm and heights ranging between 10 and 60 nm, Figure 4B.

A Model for GLP-1 Aggregation under Different Conditions. The concentration of peptide[20,21] and the presence of on-pathway oligomers[22] are both known to be important in the formation of amyloid fibrils. Increasing peptide concentration usually leads to an increase in the rate of fibrillation as observed by a reduction in lag time,[6,20] a feature that is typical of a nucleation−polymerization mechanism.[20] For GLP-1 at pH values over 8.0, an inverse relationship between lag time and peptide concentration is observed, and in this case, a simple nucleation−polymerization mechanism can be proposed where monomer (M) first associates into oligomers (O_{on}) that are on-pathway to fibril formation, Figure 5. For GLP-1, under these conditions, this is a slow nucleated

DOI: 10.1021/jacs.6b05025
J. Am. Chem. Soc. 2016, 138, 16259−16265

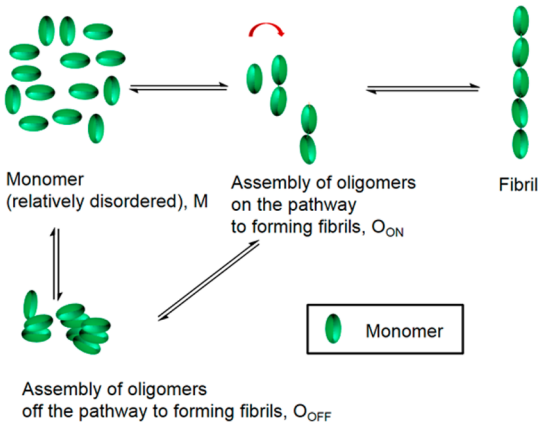

Figure 5. Proposed mechanism for GLP-1 fibril formation. There are two pathways, one in which the monomer (M) associates to form on-pathway oligomers (O_{ON}), which can convert directly into fibrils. On the second pathway, monomers can form a different oligomeric state (O_{OFF}), which is not on the direct pathway to fibril formation. The on- and off-pathway oligomers may be able to interconvert; however, the energy barriers to interconversion are likely high and the kinetics slow.

process, which leads to the specific formation of stable fibrils, which are long, stable, and twisted, Figure 4.

However, the simple nucleation−polymerization model does not explain the unusual kinetic data obtained at pH 7.5. Under these conditions, we propose a more complex model in which there is competition between the formation of on-pathway oligomers leading to fibrils and the formation of a different form of oligomer, which has to be off-pathway, Figure 5. Powers and Powers have elegantly modeled such a mechanism mathematically.[23] They have shown that, under specific kinetic conditions where a set of assumptions can be applied, a positive slope is obtained for a plot of $t_{1/2}$ versus the concentration of monomer.[23] They propose that this is an essential piece of evidence consistent with their off-pathway model.[23] This is what we observe for GLP-1 at pH 7.5, Figure 1B.

We are not the first to observe such dependence experimentally and propose a kinetic scheme in which off-pathway as well as on-pathway oligomeric species form. This has also been observed in the fibrillation of immunoglobulin light chain LEN[18] and S6 ribosomal protein.[17] In both these cases, the polypeptide starts as a globular folded protein rather than a relatively unstructured and dynamic short peptide such as GLP-1. Here, we present strong evidence that off-pathway oligomers are also populated during the fibrillation of GLP-1 at pH 7.5, highlighting this as a more general phenomenon and putting the concept proposed some years ago on firm experimental ground.

Kinetic Modeling of On- and Off-Pathway Oligomer Models. In order to verify that an off-pathway species would give rise to the difference in aggregation kinetics observed, three models for the fibrillation of GLP-1 were created within the program KinTek (see SI12 for further details). In the first model (model 1), we used a simple model of nucleation−polymerization and demonstrated that the kinetic parameter $t_{1/2}$ decreases with increasing peptide concentration as expected, Figure S11A,C. We then added an off-pathway reaction where monomer converts through monomer addition to create a series of off-pathway oligomers and added this to our starting nucleation-polymerization model to generate model 2. This model also shows a decrease in $t_{1/2}$ with increasing peptide concentration, Figure S11B,D. However, addition of the off-pathway oligomers to the reaction scheme in model 1 resulted in a delay in $t_{1/2}$ as shown in Figure S11E,F, which shows the amount of fibril formation (in terms of monomer concentration) with time at 25 and 150 μM monomer starting concentrations. The value of $t_{1/2}$ increased on addition of the off-pathway species, from 53 to 94 h at 25 μM and from 8.6 to 16 h at 150 μM monomer. These results confirm that the presence of off-pathway species results in an increase in the length of time it takes for sufficient nuclei to be formed; however, model 2 does not fully explain the results obtained for GLP-1. A third model, model 3, which was essentially the same as model 2 except an additional unimolecular step was included where monomers M interconvert with a different form of monomer, M*, and only M* forms the on-pathway oligomers required for fibril formation, was created. In this case, the dependence of the $t_{1/2}$ on initial monomer concentration switches such that it increases with increasing starting concentration, Figure S11H, as we observe experimentally for GLP-1 at pH 7.5.

Thus, our results on GLP-1 at pH 7.5 are consistent with the presence of off-pathway oligomeric species as well as a unimolecular step on-pathway to fibril formation.

Studies on rat and human isoforms of the amyloidogenic protein IAPP, associated with diabetes in humans, have recently established that various oligomeric species can be found under conditions where human IAPP forms amyloid fibrils.[24] In this case, a detailed analysis of the structure and properties of the different oligomers revealed that only the globally flexible, low-order oligomers, which did not bind ANS nor have extensive β-sheet secondary structure, were toxic to cells.[24] These results raise the interesting question of whether the on- and off-pathway oligomers that we have shown form at different pH values for GLP-1 may also have different properties including potentially different cell toxicity.

Origin of the pH-Induced Switch in Mechanism for GLP-1 Aggregation. *Net Charge on the Peptide in Its Monomeric State.* It is well established that the total charge on a peptide or protein can play an important role in determining its propensity toward aggregation.[25,26] Normally, the closer the net charge is to zero the higher propensity to aggregate, as there are little or no unfavorable electrostatic interactions to overcome to form oligomeric species and nuclei.[25]

In order to better understand our results, we used PropKa in the Schrodinger Suite to calculate the pK_a values and therefore the charge on each ionizable group in GLP-1 as a function of pH, SI13. Two structures were used as starting points: 1D0R, which is an ensemble of structures calculated from NMR experiments performed in trifluoroethanol (TFE), Figure S12A,B, and 3IOL, the structure of GLP-1 bound to its receptor. In both cases, GLP-1 is highly helical with more residues involved in α-helix formation than our far-UV CD data in aqueous buffer suggest, Figure S4. However, as no unbound structure for GLP-1 in water is available, these structures were used. Both structures gave very similar results, SI13, Figures S12 and S13. The charge on each ionizable group and the overall net charge on the peptide are shown in Figure S12C,D, respectively. The results show that there are two ionizable groups that change ionization state between pH 7.5 and 8.5: the N-terminus and the side chain of His1. The pK_a of His1 is <7, while that of the N-terminus is approximately 8. The pK_a of the N-terminus is affected by the fact that it can form hydrogen bonds with backbone amide groups as observed in the ensemble of structures generated from the NMR data, Figure S12B. On the basis of these results, we propose that the protonation state of the N-terminus plays a

DOI: 10.1021/jacs.6b05025
J. Am. Chem. Soc. 2016, 138, 16259−16265

critical role in the formation of off-pathway oligomers. When positively charged, that is, at pH values below its pK_a of approximately 8, off-pathway oligomers are favored over on-pathway oligomers. In contrast, at pH values above its pK_a, when it is uncharged, on-pathway oligomers are favored. Thus, analogs of GLP-1 that are N-terminally acetylated may well not show this unusual behavior.

Do the aggregation kinetics of GLP-1 follow the general rule that aggregation propensity increases the lower the net charge on the peptide?[25,26] The pK_a calculations suggest that GLP-1 has no overall net charge at approximately pH 5.5, Figure S12D and S13B. However, aggregation kinetics cannot be measured at this pH due to solubility problems. The net charge is predicted to increase between pH 7.5 and 8.5 due to the deprotonation of the N-terminus (from an overall net charge of approximately −1/−2 to −2/−3, Figure S12D and S13B). Experimentally, we observe an increase in the propensity of GLP-1 to form fibrils, counter to what might be expected. However, one can argue that there is an increase in the aggregation propensity of GLP-1 as its overall charge reduces, i.e., moving toward pH 5.5, but that it is an increased tendency to form off-pathway oligomers not on-pathway oligomers that would lead to amyloid fibril formation. In this regard, it is important to define specifically the aggregation state, as many such states (on- and off-pathway oligomers, fibrils, etc.) may exist.

Net Charge on the Peptide in the Oligomers. The discussion above relates to the net charge and pK_a values of ionizable groups in a highly helical, monomeric form of GLP-1. We cannot rule out that it is not the net charge of the monomer that is important, but the net charge and pK_a values of ionizable groups in the different oligomeric species that play the dominant role in the pH effects observed. Our results suggest that differences in the size and structure of the on- and off-pathway oligomers may lead to different responses to changes in pH over the range studied. In particular, the stability or the kinetics of formation/dissociation of the two oligomeric species may have different pH dependencies.

CONCLUSIONS

In conclusion, we have presented unusual aggregation kinetic data for GLP-1 at pH 7.5, where the lag time increases with increasing peptide concentration. These results indicate the likely existence of off-pathway oligomeric species, which we believe form rapidly relative to the on-pathway oligomers and which therefore act as a sink of monomers. These off-pathway oligomers will slowly dissociate and can therefore, in time, form on-pathway oligomers and ultimately fibrils. However, in addition there has to be an initial unimolecular conversion of the monomer to a different monomeric species, which can form on-pathway oligomers and ultimately fibrils. At pH 7.5, the fibrils formed by GLP-1 are short and unstable. At slightly higher pH values, pH ≥ 8.2, the aggregation kinetics of GLP-1 revert back to the simple and frequently observed nucleation−polymerization mechanism where only on-pathway oligomers are formed to any extent.

Using a number of biophysical techniques, we were successfully able to detect a range of small oligomers present in GLP-1 samples at all the pH values studied, establishing that monomeric GLP-1 is in equilibrium with either a dimer or a trimer, as well as and other slightly larger oligomeric species even in freshly prepared samples of very pure peptide. The results demonstrate that at pH 7.5, GLP-1 has a higher propensity to form oligomeric species, consistent with our proposed mechanism under these conditions where there is a rapid and nonspecific aggregation of GLP-1 into oligomers that are off-pathway.

It is also of interest to note that, under conditions where GLP-1 is very prone to forming oligomers (pH 7.5), the fibrils that it forms are short and relatively unstable. In contrast, increasing the pH by as little as 0.5 has a dramatic effect. Slightly higher pH values, where the monomeric form is more stable and therefore small oligomers much less prevalent at the beginning of the reaction, favors the formation of on-pathway oligomers and ultimately the formation of much more stable fibrils, which are long and twisted.

ASSOCIATED CONTENT

Supporting Information

The Supporting Information is available free of charge on the ACS Publications website at DOI: 10.1021/jacs.6b05025.

Supplementary results on the design and control of experiments to confirm the presence of small oligomers in freshly prepared samples of GLP-1, together with detailed aggregation kinetic data, experimental procedures for AFM imaging and the determination of fibril morphology, and supplementary figures and tables described in the paper (PDF)

AUTHOR INFORMATION

Corresponding Author

*sej13@cam.ac.uk

Notes

The authors declare no competing financial interest.

ACKNOWLEDGMENTS

The authors acknowledge Dr. Myriam Ouberai (University of Cambridge, U.K.) for her help with AFM measurements and Dr. Katherine Stott (University of Cambridge, U.K.) for her assistance in analytical ultracentrifugation experiments. We thank Dr. Adrian Podmore and Dr. Raphael J. Gubeli from MedImmune Ltd. for help with setting up the AF4 experiment. Dr. Alexander K. Buell and Georg Meisl are also acknowledged for helpful discussions (both from University of Cambridge). We also acknowledge Davide Branduardi who performed the pK_a calculations and Eric Feyant and Andrew Sparkes for interesting discussions (Schrödinger). The research was funded by MedImmune and was carried out in the Chemistry Department and the Nanoscience Centre at the University of Cambridge, U.K., and MedImmune, Granta Park, Cambridge, U.K.

REFERENCES

(1) Frokjaer, S.; Otzen, D. E. *Nat. Rev. Drug Discovery* **2005**, *4* (4), 298.
(2) Greenwald, J.; Riek, R. *Structure (Oxford, U. K.)* **2010**, *18* (10), 1244.
(3) Tycko, R.; Wickner, R. B. *Acc. Chem. Res.* **2013**, *46* (7), 1487.
(4) Eichner, T.; Radford, S. E. *Mol. Cell* **2011**, *43* (1), 8.
(5) Arosio, P.; Knowles, T. P. J.; Linse, S. *Phys. Chem. Chem. Phys.* **2015**, *17*, 7606.
(6) Cohen, S. I. A; Vendruscolo, M.; Dobson, C. M.; Knowles, T. P. J. *J. Mol. Biol.* **2012**, *421*, 160.
(7) Chiti, F.; Dobson, C. M. *Annu. Rev. Biochem.* **2006**, *75* (1), 333.
(8) Fändrich, M. *J. Mol. Biol.* **2012**, *421* (4−5), 427.
(9) Buell, A. K.; Galvagnion, C.; Gaspar, R.; Sparr, E.; Vendruscolo, M.; Knowles, T. P. J.; Linse, S.; Dobson, C. M. *Proc. Natl. Acad. Sci. U. S. A.* **2014**, *111* (21), 7671.

DOI: 10.1021/jacs.6b05025
J. Am. Chem. Soc. 2016, 138, 16259−16265

(10) Buell, A. K.; Dobson, C. M.; Knowles, T. P. J. *Essays Biochem.* **2014**, *56* (1), 11.
(11) Drucker, D. J. *Nat. Clin. Pract. Endocrinol. Metab.* **2005**, *1* (1), 22.
(12) Drucker, D. J. *Diabetes* **2015**, *64* (2), 317.
(13) Poon, S.; Birkett, N. R.; Fowler, S. B.; Luisi, B. F.; Dobson, C. M.; Zurdo, J. *Protein Pept. Lett.* **2009**, *16* (12), 1548.
(14) Jha, N. N.; Anoop, A.; Ranganathan, S.; Mohite, G. M.; Padinhateeri, R.; Maji, S. K. *Biochemistry* **2013**, *52* (49), 8800.
(15) Alvarez-Martinez, M. T.; Fontes, P.; Zomosa-Signoret, V.; Arnaud, J. D.; Hingant, E.; Pujo-Menjouet, L.; Liautard, J. P. *Biochim. Biophys. Acta, Proteins Proteomics* **2011**, *1814* (10), 1305.
(16) Nečas, D.; Klapetek, P. *Open Physics* **2012**, *10* (1), 181.
(17) Deva, T.; Lorenzen, N.; Vad, B. S.; Petersen, S. V.; Thørgersen, I.; Enghild, J. J.; Kristensen, T.; Otzen, D. E. *Biochim. Biophys. Acta, Proteins Proteomics* **2013**, *1834* (3), 677.
(18) Souillac, P. O.; Uversky, V. N.; Fink, A. L. *Biochemistry* **2003**, *42* (26), 8094.
(19) Lindgren, M.; Sörgjerd, K.; Hammarström, P. *Biophys. J.* **2005**, *88* (6), 4200.
(20) Nielsen, L.; Khurana, R.; Coats, A.; Frokjaer, S.; Brange, J.; Vyas, S.; Uversky, V. N.; Fink, A. L. *Biochemistry* **2001**, *40* (20), 6036.
(21) Powers, E. T.; Powers, D. L. *Biophys. J.* **2006**, *91* (1), 122.
(22) Lorenzen, N.; Nielsen, S. B.; Buell, A. K.; Kaspersen, J. D.; Arosio, P.; Vad, B. S.; Paslawski, W.; Christiansen, G.; Valnickova-Hansen, Z.; Andreasen, M.; Enghild, J. J.; Pedersen, J. S.; Dobson, C. M.; Knowles, T. P. J.; Otzen, D. E. *J. Am. Chem. Soc.* **2014**, *136* (10), 3859.
(23) Powers, E. T.; Powers, D. L. *Biophys. J.* **2008**, *94* (2), 379.
(24) Abedini, A.; Plesner, A.; Cao, P.; Ridgway, Z.; Zhang, J.; Tu, L.-H.; Middleton, C. T.; Chao, B.; Sartori, D.; Meng, F.; Wang, H.; Wong, A. G.; Zanni, M. T.; Verchere, C. B.; Raleigh, D. P.; Schmidt, A. M. *eLife* **2016**, *5*, e12977.
(25) Chiti, F. In *Protein Misfolding, Aggregation and Conformational Diseases: Part A: Protein Aggregation and Conformational Diseases*; Uversky, V., Fink, A., Eds.; Springer: New York, 2007; pp 47−50.
(26) Roberts, C. J. *Trends Biotechnol.* **2014**, *32* (7), 372.

DOI: 10.1021/jacs.6b05025
J. Am. Chem. Soc. 2016, 138, 16259−16265